EFFECTS OF LOW ENERGY PROTON, ELECTRON, AND SIMULTANEOUSLY COMBINED PROTON AND ELECTRON ENVIRONMENTS IN SILICON AND GaAs SOLAR CELLS

W. E. Horne, A. C. Day, and D. A. Russell
Boeing Aerospace Company
Seattle, Washington

ABSTRACT

Degradation of silicon and GaAs solar cells due to exposures to low-energy proton and electron environments and annealing data for these cells are discussed. Degradation of silicon cells in simultaneously combined electron and low-energy proton environments and previous experimental work is summarized and evaluated. The deficiencies in current solar array damage prediction techniques indicated by these data and the relevance of these deficiencies to specific missions such as intermediate altitude orbits and orbital transfer vehicles using solar electric propulsion systems are discussed.

INTRODUCTION

The concept of large solar power stations has recently increased interest in the annealing of radiation damage in space. The cost and weight of such systems make it desirable to launch them into a low earth orbit (LEO) and then transfer them to geosynchronous earth orbit (GEO). However, such a transfer, if powered by ion thruster engines, takes times on the order of a few months. This time, which is spent in the trapped proton and electron belts, results in severe electrical power output degradation. Further, other missions flying intermediate altitude orbits ($\leq$ 10,000 nmi) or elliptical orbits must pass through severe environments of electrons and protons. Thus, it is desirable to be able to anneal the cells and restore their power generating capabilities. It is the purpose of this paper to 1) look at the feasibility of such annealing, 2) consider the effects on damage level of combined environments of electrons and protons such as those encountered in such intermediate altitude orbits, 3) discuss the adequacy of current prediction techniques for predicting degradation during such missions, and 4) to assess the impact of any synergisms between simultaneous electron and proton exposures on annealing behavior and mission lifetime.

ENVIRONMENTAL

A typical transfer orbit from an initial 28° inclination to a geosynchronous orbit of 0° inclination would require approximately three months with a

variable thrust ion engine. During that time the vehicle would pass through a combined environment of vacuum, UV photons, electrons, and protons. While the UV radiation would remain constant in time (except during periods in the earth's shadow) and spectral content, the electron and proton environments vary continuously with time, position, and altitude both in intensity and energy spectrum. The actual environment varies with each orbit and during each orbit and must be determined by integration using detailed flux maps and the actual orbital history of the vehicle. However, for purposes of illustration figure 1 shows a simplified average of the integrated flux of electrons and protons as a function of altitude for a single inclination.

As a general rule the proton damage dominates for altitudes below 8,000 to 10,000 nautical miles and the electron damage dominates above that altitude (subject to variation during solar events).

For LEO to GEO orbital transfer missions most of the heavy damage to solar cells is incurred early in the mission where protons and UV, and combinations of protons, electrons, and UV are present. The proton damage, particularly the softer spectra typical of about 6,000 nmi produces a complex damage scenario inside the solar cell. Figure 2 shows a typical proton spectrum inside the solar cell as the incident spectrum is modified by shielding. As can be seen for cover glasses on the order of 2 to 3 mils thick (.012 to .018 gm/cm^2 shielding) the proton spectrum incident on the solar cell (at the interface) is quite rich in protons of energy less than 2 MeV. Particles of these energies are very damaging to solar cells. Figure 3 shows the type of gradient in damage produced across a cell due to the proton energy spectra. For example, the lower energy protons stop shortly after entering the cell and produce heavy localized damage near the ends of their tracks. The subsequent drop in intensity and effectiveness of the proton flux causes the relative amount of damage to decrease as the depth into the cell increases. It should also be pointed out that the types of defects produced and the relative concentration of each type of defect produced will also vary across the cell since these factors are energy dependent.

These observations are important not only for predicting damage level but for their impact on the annealing behavior of the cells since the annealing kinetics are different for the different defect species.

In order to better assess the impact of these environments an experimental study of low energy ($E \leq 1.5$ MeV) proton damage and annealing in both silicon and gallium arsenide solar cells has been performed at Boeing. This program has been reported in detail elsewhere (ref. 1) and, therefore is only summarized here as it pertains to evaluating missions in low and intermediate altitude orbits.

Low Energy Proton Damage and Annealing

Experiments have been performed in which 2 ohm-cm N/P MAR coated silicon solar cells were irradiated with protons of energy .25 and 1.5 MeV. The cells were irradiated at the Boeing Dynamitron accelerator. Two groups of 12 silicon cells each were exposed to 3×10^{11} and 3×10^{12} p/cm^2 respectively with 1.5

MeV protons and one group of 12 cells to 7 x 10^{11} p/cm^2 0.25 MeV protons. Isochronal and isothermal anneals were then performed to observe the annealing behavior of the cells. A similar program was conducted with GaAs cells with one group of two each exposed to 2 x 10^{13} p/cm^2 at 1.5 MeV energy and one group exposed to 1 x 10^{12} p/cm^2 at 0.25 MeV energy. The results of the isochronal annealing experiments for both types of cells are shown in figure 4. These curves show evidence of the break up of several defect species in the silicon cells. Some of these species appear to be products of new combinations of defects and impurities pairing as the original defects break up and their constituents migrate away from their original sites (refs. 1, 2). The new species usually have different electrical degradation properties from their predecessors and are considerably different in their annealing properties. The relative amounts of the different defect species also appear to be rather strong functions of the incident proton energy.

The isochronal anneals of the GaAs cells also show structure indicating the annealing of multiple defect species. However, they do not show the reverse annealing as in the case of silicon cells. This is probably indicative of less interaction between the defects and impurities in GaAs cells.

Figure 5 shows typical isothermal annealing behavior for both silicon and GaAs cells. In both cases, the curves show evidence of the recovery of multiple species having different annealing time constants corroborating the observations of the isochronal anneals.

Other significant observations of this study were that 1) in the silicon cells both the rate and extent of recovery are functions of proton energy and of damage level or fluence, 2) recovery appears to be more rapid and more complete when the cells are heated rapidly above 400°C, with recovery levels of 96 percent of maximum power in times on the order of five minutes being typical, 3) the rate and extent of recovery under a given set of conditions varies widely between cells with very similar initial electrical characteristics and radiation degradation responses as a function of fluence. For the GaAs cells the rate and extent of recovery was also a function of incident proton energy.

Combined Environments of Electrons, Protons, and UV Radiation

Another complexity that needs to be considered for orbits $\leq$ 10,000 nmi is that of synergistic effects between simultaneous environments of UV, electrons, and protons. In the past, at least three experiments have been performed on solar cells with combined environments of these three constituents. These experiments are summarized in table 1.

The first two experiments summarized in table 1 are in general agreement in that they both experienced combinations of electrons, protons, and UV radiation and both showed less damage than would be expected for the linear sum of the defects produced by the particulate beams taken separately. A typical difference is illustrated in figure 6. However, the third experiment summarized in table 1 showed significantly different results in that a rather strong synergism was reported between the electron and proton environments as illus-

trated in figure 7. If one examines the conditions of the three experiments some significant differences are noted that could account for the seemingly conflicting results. In the third experiment the synergism between the electron and proton environments was a rather strong function of the ratio of electron and proton fluxes. In the first two experiments the proton beams were spread over the sample fields by rastering, or scanning, the beams in the vertical and horizontal planes. This resulted in an instantaneous proton flux much higher than the average number reported, or a much lower ratio of electron flux to proton flux than was reported. Looking at the results of the third experiment, a low ratio of electrons to protons shows little or no synergism so that the results may in fact not be in conflict at all. It should be further pointed out that in both the first and third experiments linear accelerators were used to supply the electrons. These machines operate in a single or repetitive pulsed mode but do not supply a continuous beam of electrons. In the second experiment a continuous field of scattered Compton electrons was present but the proton beam was rastered. Thus it can be concluded that none of the experiments have really been a satisfactory simulation.

Summary of Impact on Mission Performance

If one considers the synergism of figure 7 a possible mechanism could be that a high level of electrons during the proton exposure tends to break up the initial defect complexes produced by the protons allowing the formation of more electrically degrading complexes in much the same way observed for the reverse annealing of low energy proton damage at moderate temperature. If this is the true mechanism, or if different defect species are being formed, then the annealing kinetics of the damage would be altered considerably. For example, it was observed in the low energy proton damage annealing experiments that when cells were rapidly heated above 400°C then less of the secondary or daughter defects were produced during the annealing process and the annealing progressed more rapidly and completely than at lower temperatures or during isochronal anneals which slowly stepped the cells to > 400°C through a series of incremental temperature steps. Thus, if the combined environments produce the equivalent of the reverse anneal observed in the isochronal anneal experiments then both the rate and the extent of final annealing would be affected.

Thus, it can be seen that the complexity of the damage produced across the thickness of a solar cell by a spectrum of low energy protons and the possibility of synergisms can radically alter the behavior of arrays during long term missions in intermediate and low altitude orbits both in terms of initial degradation and in the feasibility of annealing of the damage.

CONCLUSIONS

From the above observations it is concluded that low-energy proton damage and annealing is not sufficiently understood or characterized to permit accurate engineering evaluations of large-scale power supply performance in orbits $\leq$ 10,000 nmi. More work is required in the area of understanding basic mechanisms of annealing and the results of repetitive irradiate-anneal cycles.

It is also concluded that the area of synergisms between electron, low-energy proton, and UV environments has not been adequately explored to permit certainty in engineering design of power systems and annealing cycles to optimize mission performance.

REFERENCES

1. Day, A. C., Horne, W. E., and Arimura, I., "Proton Damage Annealing for Use in Extended Life Solar Arrays," to be published in IEEE Transactions on Nuclear Science, Volume 27, No. 6, December 1980.

2. Weinberg, I. and Swartz, C. K., "Origin of Reverse Annealing in Radiation Damaged Silicon Solar Cells," Appl. Phys. Lett. 32(8), 1980.

3. Arndt, R. A., Bernard, J, and Reulet, R., "Effects of Simultaneous Ultraviolet, Electron, and Proton Irradiation of Silicon Solar Cells," IEEE Photovoltaic Specialist's Conf. Proceedings, 1975.

4. Horne, W. E., Madaras, B. V., and Greegor, R., "Real Time Space and Nuclear Effects on Solar Cells (Accelerated Evaluation Methods)," AFAPL-TR-72-69, 1974.

TABLE 1. SUMMARY OF COMBINED ENVIRONMENT EXPERIMENTS ON SOLAR CELLS

SOURCE OF DATA	DESCRIPTION OF ENVIRONMENTS									TYPES OF CELLS EXPOSED	RESULTS OBSERVED
	PROTONS			ELECTRONS			UV				
	ENERGY	FLUX (p/cm^2-s)	EXPOSURE TECHNIQUE	ENERGY	FLUX (e/cm^2-s)	EXPOSURE TECHNIQUE	ENERGY	FLUX	EXPOSURE TECHNIQUE		
Arndt, et al. (ref. 3)	2.5 MeV	2×10^7 2×10^8 (average)	Rastered Beam	2.0 MeV	2×10^{10} 2×10^{11}	Scattered Pulsed Field (rep. rate unk.)	Unfiltered Xenon Lamp	1 UV Sun (average)	Variable Intensity	1 Ω-cm Float Zone 10 Ω-cm Float Zone 10 Ω-cm Crucible N/P	• No Synergism Between Electron and Proton Environments • Less Damage in Cells Exposed to UV Plus Particulate Radiation Than in Those Exposed to Particles Only
Horne, et al. (ref. 4)	0.1 MeV	1.2×10^5 (average)	Rastered Beam	1.33 MeV (average)	9.1×10^6	Scattered Compton Electron Continuous Field	Quartz Iodide Lamps	~ 1 UV Sun (average)	Continuous	10 Ω-cm Crucible N/P Crucible P/N (lithium) Float Zone P/N (lithium)	• Less Damage Than Expected Based on Linear Sum of Particulate Environments Similar to Above Experiment Where UV Radiation Was Present
Horne, et al. (ref. 4)	0.26 MeV	$\sim 10^7$ $\sim 10^8$	Scattered Continuous Field	10 MeV	$\sim 10^{10}$	Scattered Pulsed Field (rep. rate 15 p/s)	None	———	———	10 Ω-cm Crucible N/P Crucible P/N (lithium) Float Zone P/N (lithium)	• Synergism Observed Between Electron and Proton Environment • More Damage Than Would Be Expected From Linear Sum of Separate Environments • Synergism a Function of Ratio of Electron Flux to Proton Flux

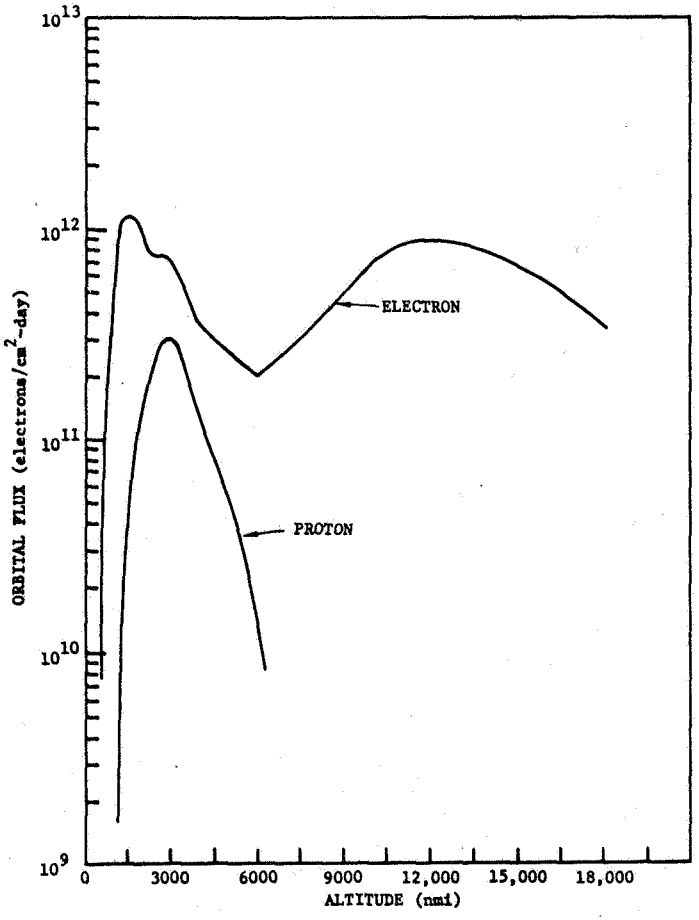

FIGURE 1. VARIATION OF ORBITAL FLUX WITH ALTITUDE

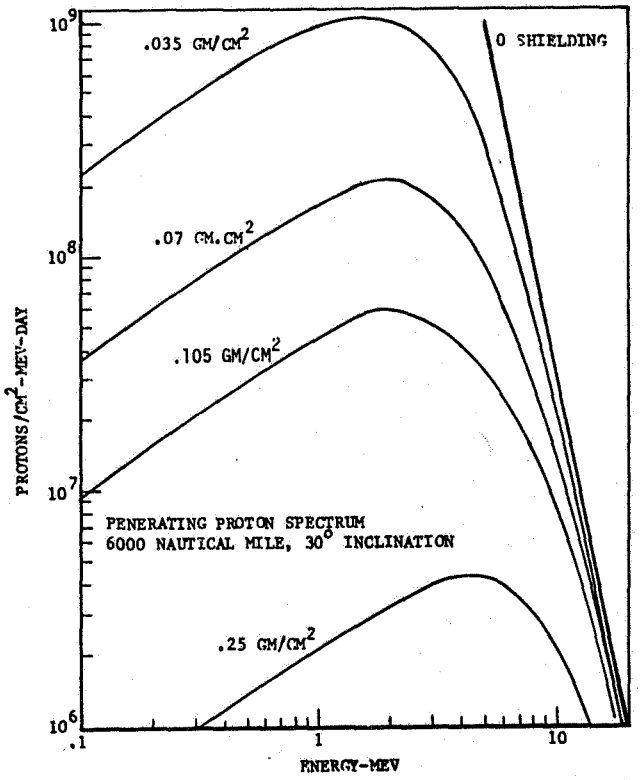

FIGURE 2. TYPICAL MODIFIED SPECTRUM INSIDE SOLAR CELL STRUCTURE (6000 nmi, 30° INCLINATION)

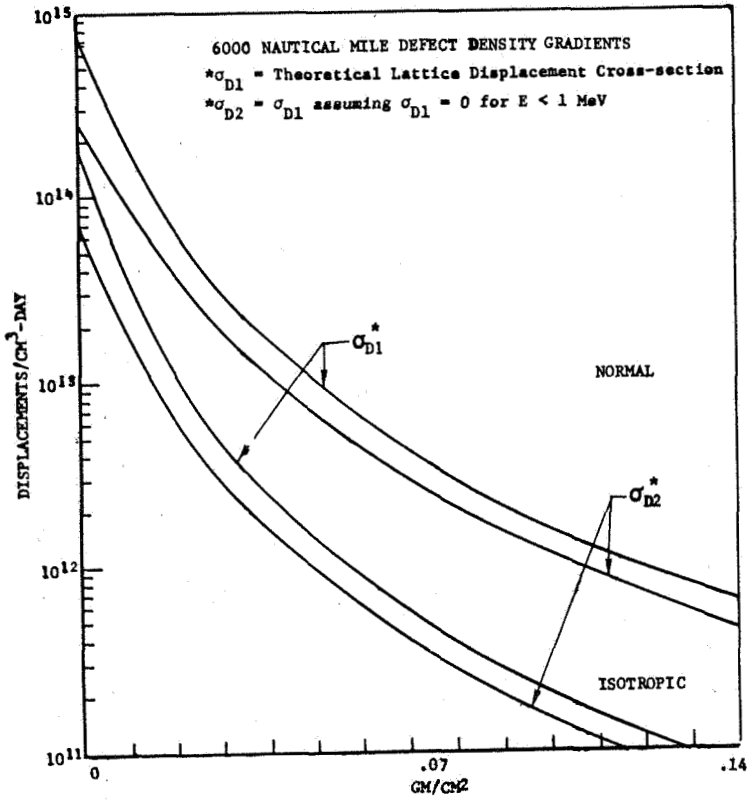

FIGURE 3. TYPICAL DISPLACEMENT DENSITY GRADIENT INSIDE SOLAR CELL DUE TO SPACE SPECTRUM

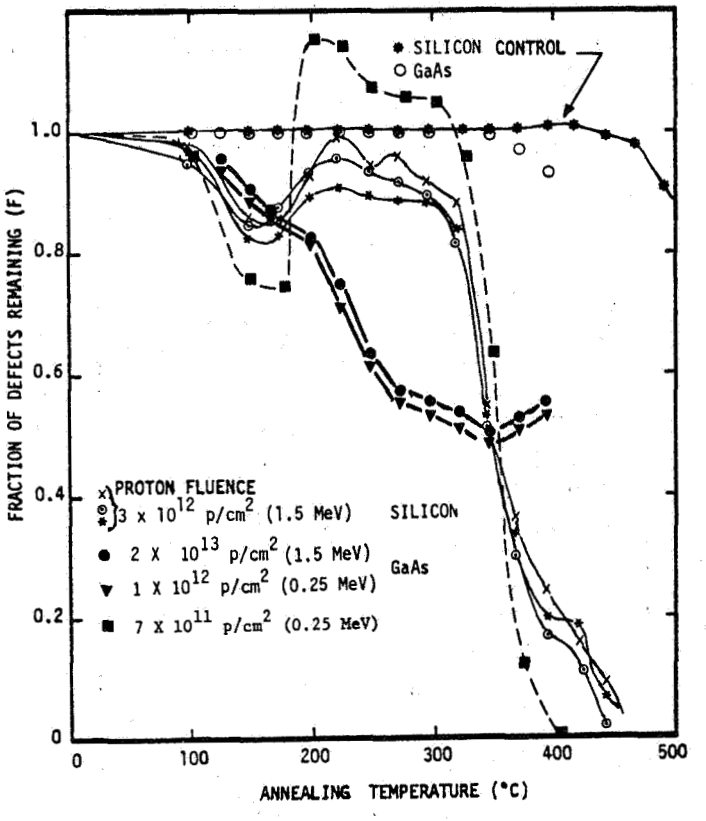

FIGURE 4. ISOTHERMAL ANNEALING DATA FOR SILICON AND GaAs SOLAR CELLS

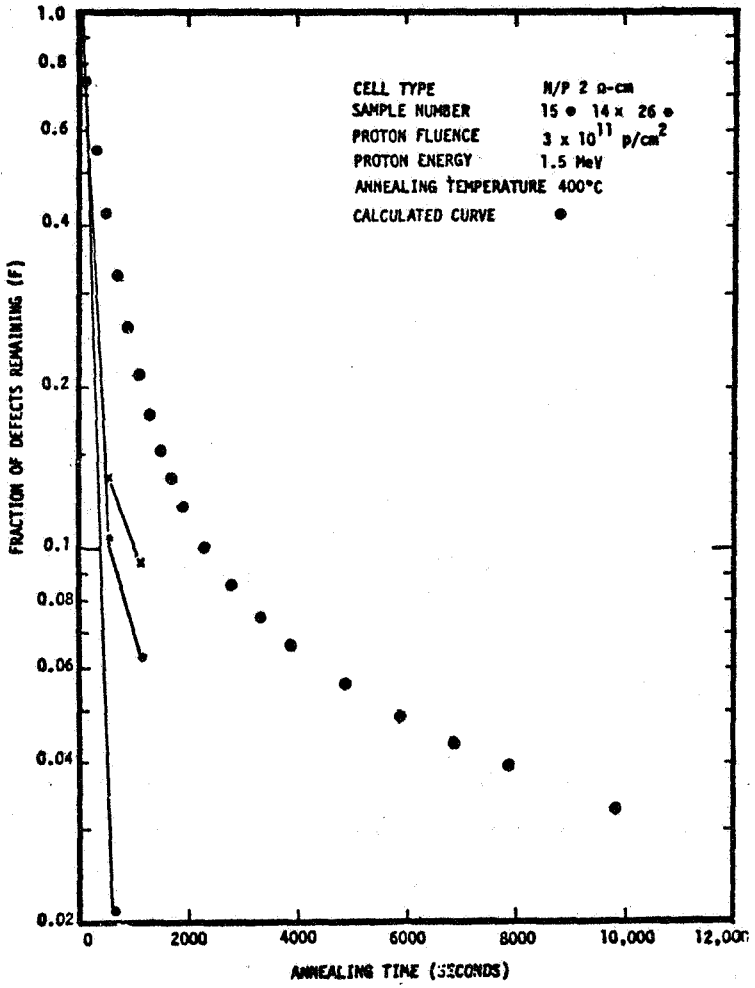

FIGURE 5a. ISOTHERMAL ANNEAL OF SILICON CELLS FOLLOWING 3 x 10^{11} p/cm^2

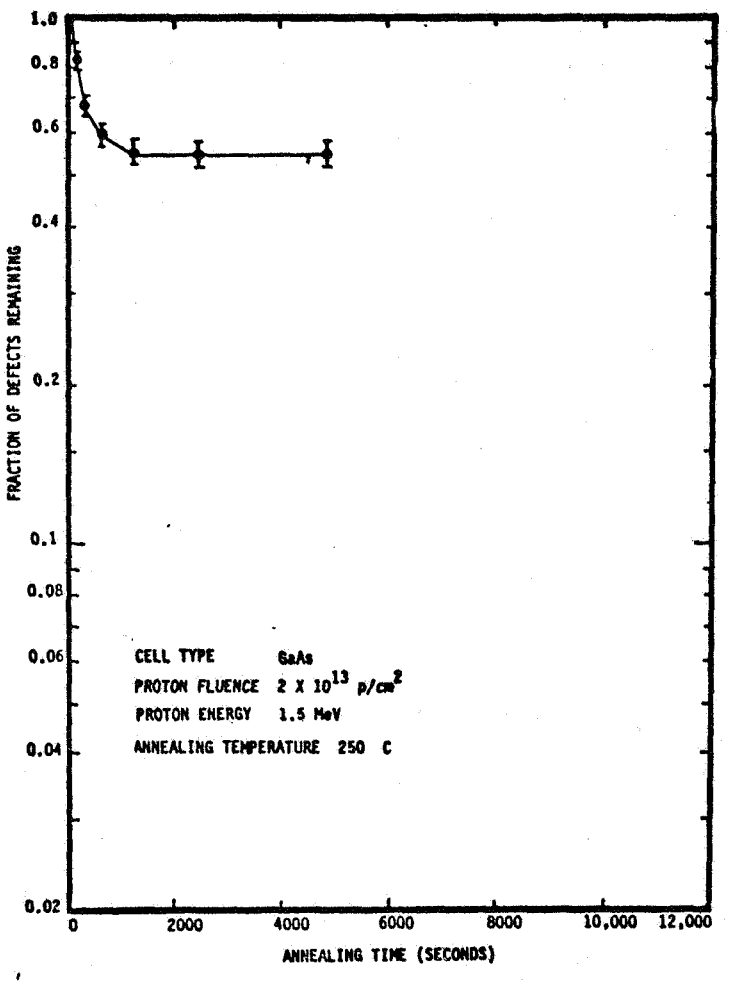

FIGURE 5b. ISOTHERMAL ANNEAL OF GaAs CELLS

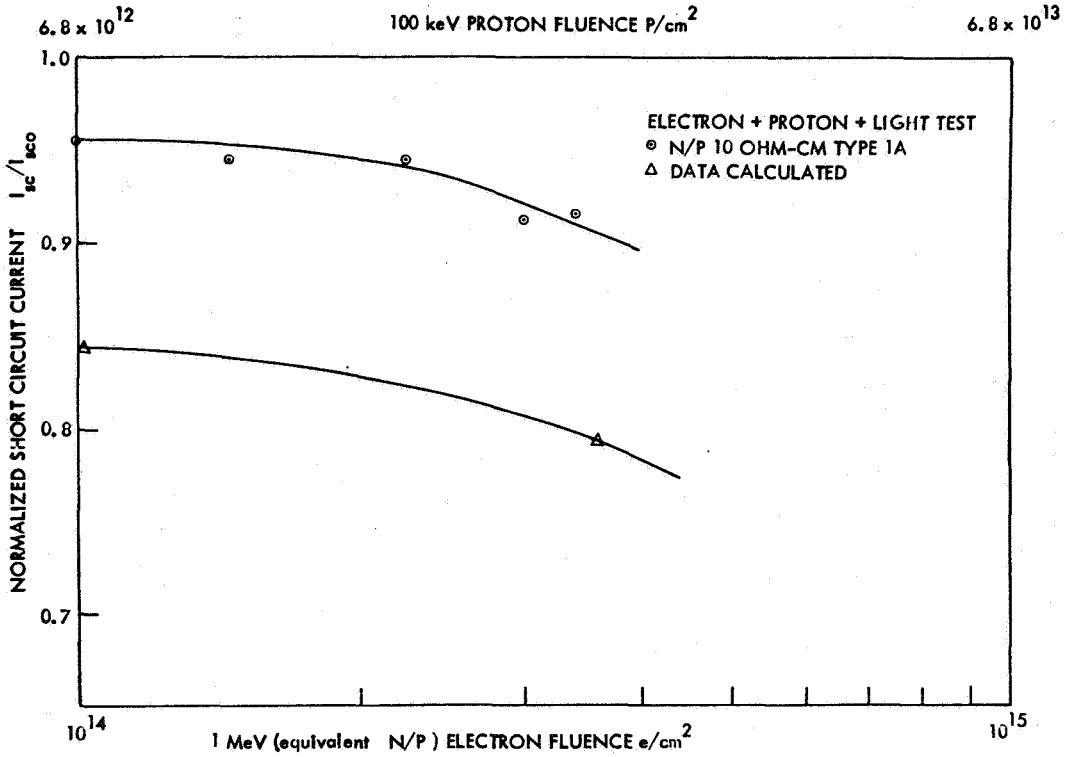

FIGURE 6. COMPARISON OF CALCULATED VERSUS MEASURED DATA FOR COMBINED ENVIRONMENT REAL-TIME TEST

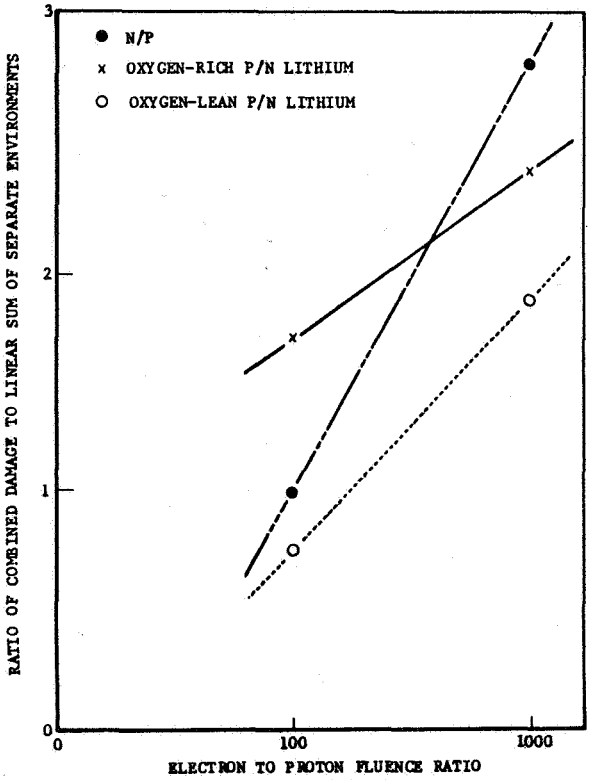

FIGURE 7. RATIO OF ENHANCED COMBINED EFFECTS DAMAGE TO LINEAR SUM OF SEPARATE DAMAGE COMPONENTS VERSUS THE ELECTRON TO PROTON FLUENCE RATIO DURING THE COMBINED TESTS